Collision-Induced Dissociation in Quadrupole Ion Traps: Application of a Thermal Model to Diatomic Ions

Douglas E. Goeringer,*,† Douglas C. Duckworth,† and Scott A. McLuckey‡

Chemical and Analytical Sciences Division, Oak Ridge National Laboratory, Oak Ridge, Tennessee 37831-6365, and Department of Chemistry, Purdue University, West Lafayette, Indiana 47907-1393

Received: October 31, 2000; In Final Form: January 4, 2001

Dissociation of the tantalum oxide cation, a strongly bound diatomic, is simulated for the multiple-collision environment of a quadrupole ion trap mass spectrometer using a model based on thermal unimolecular reaction theory. The intact diatomic ion is assigned a specific internal temperature at which it undergoes collisional activation and deactivation during a random walk in energy space. Collisional energy transfer is assumed to proceed via independent vibrational and rotational processes, as described by the refined impulse approximation and exponential transition probability, with dissociation occurring when the vibrational energy exceeds the rotational-energy-dependent barrier for dissociation. Processing the data from many such random walks yields the simulated dissociation kinetics and time-dependent internal energy distribution of an ion population at the specified internal temperature. Comparison of experimental dissociation rates with those obtained via simulations performed over a series of temperatures enables prediction of internal temperatures and corresponding internal energy distributions for tantalum oxide ion populations undergoing resonance excitation. Although the simulations indicate that rotational-energy transfer can lead to significantly higher dissociation rates than those associated with purely vibrational-energy transfer, the results obtained in this study suggest that ion internal temperatures in the tens of thousands of degrees are required nonetheless to dissociate a strongly bound diatomic ion such as tantalum oxide, and the experimental data demonstrate that resonance excitation in a quadrupole ion trap can achieve the necessary temperatures.

Introduction

Quadrupole ion traps, as currently used in chemical research, are typically operated with a low-mass buffer gas, usually helium, present at a pressure of roughly 1 mTorr. One of the primary roles for the buffer gas is deceleration of ions via momentum transfer collisions, the overall purpose being to facilitate capture of ions injected from external ion sources[1−4] and to thermalize and collapse ion populations to the center of the trapping volume. Another important function of the buffer gas is serving as the target species for collisional activation experiments; in this role, transfer of kinetic energy to internal energy is the important underlying phenomenon. A variety of techniques for accelerating ions in ion traps for collisional activation purposes have been reported.[5−12] These include, among others, accelerating a parent ion at or near its fundamental *z*-dimension secular frequency by applying a sine wave to the end-cap electrodes [5] (i.e., the so-called resonance excitation technique), placing an ion near to the edge of the stability diagram so that the ion is accelerated by the radio frequency drive voltage,[7−9] and applying a low-frequency signal to the end caps.[12]

A wide range of ions, extending from strongly bound diatomic ions[13] to multiply charged proteins with masses exceeding 10 kDa,[14−16] has been dissociated using collisional activation in quadrupole ion traps. Despite the relatively modest center-of-mass collision energies (usually much less than 5 eV) associated with individual collisions of heavy ions and light targets, the multiple-collision nature of ion trap collisional activation makes possible the dissociation of a wide range of ions. Ion trap collisional activation and the blackbody infrared-dissociation technique used in the Fourier transform ion cyclotron resonance (FTICR) mass spectrometer[17,18] are analogous in that both entail multiple activation/deactivation processes. In the virtually collision-free environment of the FTICR mass spectrometer, the relative rates of infrared photon absorption and emission (i.e., activation and deactivation) as compared with unimolecular dissociation determine the ion internal energy distribution and overall dissociation rate.[17−21] In contrast, nearly all ion acceleration-based methods in the relatively high-pressure environment of the ion trap involve at least hundreds of ion−neutral collisions and relatively long periods over which ion acceleration is typically effected (10−1000 ms).[22] Consequently, dissociation kinetics and internal energy distributions are dependent upon the ratio of unimolecular dissociation rates to rates of collisional activation and deactivation, rather than photon absorption and emission. Therefore, we have developed a model based on thermal unimolecular reaction theory to describe the kinetics of ion trap collision-induced dissociation (CID) effected via resonance excitation.[23,24] It is interesting to note that for both dissociation methods conditions can be established where ion activation and deactivation rates can greatly exceed unimolecular dissociation rates.[17,25] In this situation, referred to as the rapid energy exchange condition,[18] dissociation rates follow the Arrhenius equation. At the opposite extreme, decomposition rates are determined by the excitation rate over

* To whom correspondence should be addressed. Phone: (865)574−3469. Fax: (865)576-8559. E-mail: goeringerde@ornl.gov.
† Oak Ridge National Laboratory.
‡ Purdue University.

10.1021/jp0040289 CCC: $20.00
Published on Web 02/07/2001

the barrier for vibrational dissociation, a situation that applies to diatomic ions.

It is desirable to understand the relationship between the experimental conditions used in ion trap collisional activation, such as with the resonance excitation technique, and the effective ion temperatures to which diatomic ions can be raised. We have approached the problem by simulating CID of the tantalum oxide cation, a strongly bound metal oxide ion for which ion trap dissociation rates during resonance excitation have been determined experimentally, under thermal conditions. That is, parent ions are initially assigned a specific internal temperature which, in turn, leads to the dissociation rate expected for an ion present in a buffer gas at the internal temperature used for the simulation. The internal temperatures achievable are then estimated via the comparison of simulated dissociation rates with experimentally determined dissociation rates. It is necessary to resort to such a simulation for strongly bound diatomic ions because buffer gas temperatures required to dissociate them at rates on the order of $10-100\ s^{-1}$ are extremely difficult to access experimentally. Elements of our previously reported model for ion trap CID form the basis for the simulations. In addition, rotational excitation is also considered in this work because rotational energy content of a diatomic ion can alter significantly the vibrational dissociation barrier and thereby affect calculated dissociation rates. Our approach differs from other simulations of diatomic dissociation[26,27] in that it provides estimates of ion internal temperatures for a prototypical strongly bound diatomic ion, complementing a recently reported work which has correlated ion activation conditions and effective ion internal temperatures for a relatively large polyatomic ion, protonated leucine enkephalin.[28] The results reported herein are highly relevant to understanding the chemical and physical phenomena underlying the use of the ion trap as a tool in elemental mass spectrometry,[29−35] wherein the destruction of polyatomic ion interferences is often desirable.

Experimental Section

Experimental results described here were collected using a quadrupole ion trap mass spectrometer coupled with a pulsed direct current glow discharge (GD) ionization source. Details of the instrumental configuration[28] and CID methodology[36] have been previously described. The instrument is a Teledyne 3DQ ion trap modified for injection of externally generated GD ions. A tantalum metal pin was used as the cathode, generating Ta^+ ions which were sampled into the ion trap. TaO^+ formation resulted from reactions with adventitious gases within the analyzer region.

Collisional activation data were acquired using Ne (99.995%) buffer gas admitted to the vacuum system to bring the total background pressure in the ion trapping volume to 0.5 mTorr. Neon was also used as the GD support gas. The typical experimental sequence involved an ion accumulation period (5 ms), a Ta^+ reaction period ($\sim$ 25ms), a parent ion isolation step (5 ms), a 25 ms ion cooling period at $q_z = 0.2$, a resonance excitation of a mass-selected ion, and mass analysis by mass-selective instability.[37] The GD source was pulsed such that the pulse width defined the ion accumulation period. Ion isolation was effected by mass selective instability.[38,39] Less than unit mass resolution in ion isolation was sometimes used, but single-frequency resonance excitation was selective for a narrower range of mass to charge. In all cases, experiments were performed that activated a single parent ion type. The amplitude of the resonance excitation voltage, which was applied in dipolar fashion to the end-cap electrodes, and the q_z value for the parent ion are indicated in the text.

Simulations were performed on a Macintosh PowerPC G3 with procedures written in Mathcad PLUS 6 for Macintosh (MathSoft Inc., Cambridge, MA).

Theory

Description of the Model for Collisional Activation. Many of the elements of the model used in this work have been described in detail previously.[23,24] The model, based on thermal unimolecular reaction theory, is summarized briefly here primarily to point out the assumptions used and the criteria that must be met to maximize their validity. The assumptions used are as follows:

1. Ion number densities are much lower than neutral number densities so that ion−ion collisions can be ignored.

2. The ion power absorption during ion acceleration is sufficiently low so that a steady-state ion kinetic energy distribution can be established whereby ion acceleration by the oscillating electric field is balanced by deceleration via collisions.

3. Absorption and emission of light by the ions is a far less important energy-transfer process than collisional energy transfer under the experimental conditions used here and can therefore be ignored.

4. The unimolecular dissociation rate of ions with internal energies equal to or greater than the critical energy for dissociation greatly exceed the rates for collisional activation and relaxation so that the sudden-death approximation can be used to model dissociation.

5. Ions are stored in a pure quadrupolar electric field so that the ion secular frequency is independent of oscillatory amplitude (i.e., no higher order field components that give rise to nonlinearity in ion acceleration are present).

Experimental conditions can be established where assumptions 1−4 are valid. For example, ion number densities are always at least 5 orders of magnitude lower than that of the buffer gas (assumption 1). Assumption 2 is likely to be valid under conditions in which 100% of the parent ion loss can be accounted for by the appearance of product ions. The study of diatomic ions ensures that assumptions 3 and 4 are valid. However, assumption 5 is clearly not valid for most ion traps commonly used in chemical research. Such ion traps are usually modified intentionally to incorporate higher order fields. This model does not take into account the effect of such fields on the ion acceleration process and is one reason the ion acceleration process associated with resonance excitation was not included in this simulation. Rather, an initial parent ion internal temperature was assigned to the parent ions for determination of dissociation kinetics. By assigning a parent ion internal temperature to the ions, any errors associated with assumption 2 are also obviated.

Master Equation. A general picture of the dissociation of ions, AB^+, via energetic collisions with atomic neutral species, M, can be represented by the Lindemann mechanism for thermal unimolecular reactions, in which the collisional energy transfer (eq 1) and dissociation (eq 2) steps are treated as two distinct processes.

$$AB^+ + M \underset{k_{deact}}{\overset{k_{act}}{\rightleftharpoons}} AB^{+*} + M \qquad (1)$$

$$AB^{+*} \xrightarrow[k_d]{} A^+ + B \qquad (2)$$

k_{act} and k_{deact} are the rate constants for activation and deactivation of the energized ion (i.e., an ion having sufficient energy to

fragment) AB^{+*}, respectively, and k_d is the unimolecular dissociation rate coefficient for AB^{+*}. Using the steady-state assumption for AB^{+*}, an expression can be written for the overall dissociation rate of AB^+

$$\frac{d[AB^+]}{dt} = -k_{diss}[AB^+] \tag{3}$$

where the observed dissociation rate constant k_{diss} is given by eq 4:

$$k_{diss} = \frac{k_{act}[M]}{k_{deact}[M] + k_d} k_d \tag{4}$$

Lindemann theory assumes that every $AB^{+*}-M$ collision results in deenergization (strong collision assumption), so that, $k_{deact}[M]$ is equal to the collision frequency ω. Furthermore, k_d for diatomic ions is on the order of vibrational frequencies (ca. 10^{13} s^{-1}) and is thus much larger than ω. Thus, the expression for k_{diss} can be rewritten

$$k_{diss} = k_{act}[M] \tag{5}$$

indicating that collisional activation is rate-determining. Line-of-centers collision theory stipulates that k_{act} is the frequency of collisions for which the center-of-mass kinetic energy is greater than or equal to E_0 (the critical dissociation energy), $k_{act} = Z \exp(-E_0/kT)$, where Z is the gas-kinetic collision number. However, this picture assumes all ions reside initially in the vibrational ground state and cannot account for dissociation that results from stepwise excitation.

Considering the overall mechanism for activation/deactivation as a multistep process gives

$$AB^+(E) + M \underset{R(E',E)}{\overset{R(E,E')}{\rightleftharpoons}} AB^+(E') + M \tag{6}$$

$$AB+(E') \xrightarrow[k_d(E')]{} A^+ + B \tag{7}$$

where $R(E;E')$ is the rate coefficient for collisional energy transfer from energy E to E'. A coupled set of differential equations, referred to as the master equation, can then be constructed from eqs 6 and 7 to describe the time-dependent population of the individual energy levels

$$\frac{d[AB^+(E')]}{dt} = \omega \sum_E ([AB^+(E)]P(E;E') - [AB^+(E')]P(E';E)) - k_d(E')[AB^+(E')] \tag{8}$$

where $R(E;E')$ has been expressed in terms of the energy-transfer probability $P(E;E')$ according to eq 9:

$$P(E;E') = \frac{[M]R(E;E')}{\omega} \tag{9}$$

Realizing that at steady-state $[AB^+(E)] \approx 0$ above E_0 for diatomics and that the energy-dependent unimolecular dissociation rate coefficient $k_d(E')$ is zero below E_0 and substituting for $d[AB^+]/dt$ according to eq 3 gives eq 10:

$$-k_{diss}g(AB^+(E')) = \omega \sum_{E<E_0} g(AB^+(E))P(E;E') - \omega g(AB^+(E')) \tag{10}$$

where $g(AB^+(E)) = [AB^+(E)]/[AB^+]$ is the normalized population density at energy E. Thus, the macroscopic dissociation rate constant k_{diss} and the normalized time-dependent population of the individual energy levels can be obtained via simulation of the microscopic energy-transfer processes.

Collisional Energy-Transfer Probability Function. Of the several functional forms for the energy-transfer probability function that have been described,[40] the exponential down-step probability function for inefficient colliders $P_{exp}(E;E')$ is perhaps most appropriate for the small energy transfers expected for TaO^+ collisions with the monatomic collider in this work, Ne:

$$P_{exp}(E;E') = \frac{\exp\left[\frac{-(E-E')}{\alpha}\right]}{C}, \quad E > E' \tag{11}$$

$$= \frac{\exp\left[\frac{-(E'-E)}{\beta}\right]}{C}, \quad E < E' \tag{12}$$

α is the average downward energy transfer in an ion−neutral collision, and the average up-step size β at ion internal temperature T_{int} is given by

$$\beta = \frac{\alpha k T_{int}}{\alpha + kT_{int}} \tag{13}$$

The normalization factor C

$$C = \frac{1 + \alpha/kT_{int}}{\alpha(2 + \alpha/kT_{int})} \tag{14}$$

is obtained from the statistical mechanical constraint of microscopic reversibility, where the density of states is assumed to be independent of the energy for diatomics[41].

Magnitude and Functional Form of Collisional Energy-Transfer Parameters. A key issue in simulating CID kinetics is the determination of the magnitude and functional form for the parameters α and β, because they have a direct effect on ion deactivation and activation probabilities and the associated rate coefficients for collisional energy transfer. An approximate solution to the problem of translational−vibrational (T−V) energy exchange during a zero impact parameter (i.e., collinear) collision between an atom and a diatomic (harmonic) oscillator, such as that indicated in eq 1, has been derived by several workers using classical dynamics. However, the approximate solution ΔE_{apx} does not converge to the expected impulse limit as the M−AB interaction time becomes very small compared to the AB vibrational period. The refined impulse approximation (RIA),[42,43] a modification of the classical dynamical approximation, gives higher accuracy and is correct in the impulse limit. The RIA expression for maximum collisional energy transfer ΔE_{RIA} is

$$\Delta E_{RIA} = 4 \frac{m_M m_A m_B m_{total}}{(m_M + m_{target})^2 m_{AB}^2} KE_{COM} f(\xi) \tag{15}$$

where the mass of species x is denoted by m_x, m_{target} refers to the specific atom of the diatomic undergoing collision with M, $m_{total} = m_M + m_{AB}$, and KE_{COM} is the center-of-mass (COM) kinetic energy. The function $f(\xi)$, which accounts for deviation from the impulse limit, is discussed further below.

The relationship between ΔE_{apx} and ΔE_{RIA} is

$$\frac{\Delta E_{apx}}{\Delta E_{RIA}} = \frac{(m_M + m_{target})^2 {m_{AB}}^2}{{m_{target}}^2 {m_{total}}^2} \quad (16)$$

Furthermore, extensive numerical calculations for T−V energy exchange have been performed by Kelley and Wolfsberg;[44] their results indicate that the exact energy transfer ΔE_{num} is smaller than the approximate solution by a factor

$$\frac{\Delta E_{apx}}{\Delta E_{num}} = \exp\left[1.685 \frac{m_M m_{\overline{target}}}{m_{target}(m_M + m_{AB})}\right] \quad (17)$$

where $m_{\overline{target}}$ represents the atom of the diatomic not undergoing collision with M. Thus, dividing eq 16 by eq 17 gives a factor $F = \Delta E_{num}/\Delta E_{RIA}$ which can be used to give corrected RIA values ΔE_{Corr}. Averaging over all possible collision parameters then yields the average (corrected) energy transferred $\langle \Delta E_{Corr} \rangle$ given in eq 18

$$\langle \Delta E_{Corr} \rangle = 2 \frac{m_M m_A m_B m_{total}}{(m_M + m_{target})^2 {m_{AB}}^2} \langle KE_{COM} \rangle f(\xi)\, F \quad (18)$$

where angle brackets denote average values.

The total kinetic energy KE_{total} of ions moving through a gas under the influence of an electric field is comprised of terms related to directed, $KE_{directed}$, and stochastic, $KE_{stochastic}$, motion:

$$\langle KE_{total} \rangle = \langle KE_{directed} \rangle + \langle KE_{stochastic} \rangle \quad (19)$$

$KE_{stochastic}$ represents that part of KE_{total} which is available for conversion to internal energy and is thus equal to KE_{COM}; T_{eff} is the ion temperature associated with that stochastic motion, so that, $\langle KE_{COM} \rangle = {}^3/_2 kT_{eff}$. Substitution for $\langle KE_{COM} \rangle$ in eq 18 yields

$$\langle \Delta E_{Corr} \rangle = 3 \frac{m_M m_A m_B m_{total}}{(m_M + m_{target})^2 {m_{AB}}^2} kT_{eff}\, f(\xi)\, F \quad (20)$$

The function $f(\xi)$ is given by eq 21

$$f(\xi) = \xi^2 \operatorname{csch}^2(\xi), \quad \xi = \frac{2\pi^2 \nu L}{v_{M-AB}} \quad (21)$$

where ξ is the so-called adiabaticity parameter, ν is the AB vibrational frequency, L is a characteristic distance for the neutral-target atom interaction ($\sim$ 0.2 angstroms), and v_{M-AB} is the relative diatomic-neutral velocity. The impulse limit is approached (i.e., $\xi \rightarrow 0$ and $f(\xi) \rightarrow 1$) as the collision duration becomes short compared to the vibrational period ($L/v_{M-AB} \ll 1/\nu$). Using the definition $KE_{COM} = (\mu_{M-AB} {v_{M-AB}}^2)/2$, where μ_{M-AB} is the reduced mass of M and AB, gives the relative diatomic-neutral velocity:

$$v_{M-AB} = \sqrt{\frac{3kT_{eff}}{\mu_{M-AB}}} \quad (22)$$

Because KE_{COM} is directly related to T_{eff}, the function $f(\xi) \rightarrow 1$ as $T_{eff} \rightarrow \infty$.

Associating $\langle \Delta E_{Corr} \rangle$ with vibrational energy up-steps allows the following expression to be written for β_{vib}:

$$\beta_{vib} = 3 \frac{m_M m_A m_B m_{total}}{(m_M + m_{target})^2 {m_{AB}}^2} kT_{eff}\, f(\xi)\, F \quad (23)$$

Furthermore, an estimate of the vibrational energy down-step parameter can be obtained from α by solving eq 13 for α to give eq 24:

$$\alpha_{vib} = \frac{\beta_{vib} kT_{int}}{kT_{int} - \beta_{vib}} \quad (24)$$

Substituting for β_{vib} in eq 24 using eq 23 and realizing that for diatomic-atomic collisions (assuming no electronic excitation of the target) T_{int} is equal to T_{eff} gives the expression for α_{vib} below:

$$\alpha_{vib} = \frac{3 \dfrac{m_M m_A m_B m_{total}}{(m_M + m_{target})^2 {m_{AB}}^2} kT_{eff}\, f(\xi)\, F}{1 - 3 \dfrac{m_M m_A m_B m_{total}}{(m_M + m_{target})^2 {m_{AB}}^2} f(\xi)\, F} \quad (25)$$

Rotational-Energy Effects. Although the above discussion assumes that the energy levels are associated with vibrational motion, for diatomics, the consideration of rotational degrees of freedom is important as well. For decompositions involving simple bond breaking without a recombination barrier, such as diatomic dissociations, conservation of angular momentum requires rotational energy to be released into vibrational motion as interatomic distance increases. The result is that the threshold energy for vibrational dissociation becomes a (decreasing) function of (increasing) rotational energy E_{rot} (eq 26):[41]

$$E_0(E_{rot}) = E_0\left[1 - \frac{E_{rot}}{E_0} + \sqrt{\frac{2}{27}}\left(\frac{E_{rot}}{E_0}\right)^{3/2}\right] \quad (26)$$

enabling decomposition to occur over a range of vibrational energies less than E_0. Furthermore, although angular momentum doesn't vary during the period between collisions, it is altered as the result of collisions, thereby inducing a corresponding change in the rotational energy. Rewriting eq 8 to take both vibrational- and rotational-energy changes into account yields a two-dimensional master equation involving a unimolecular dissociation rate coefficient and energy-transfer probabilities which are dependent on both vibrational and rotational energy [i.e., $k_d(E) = k_d(E_{vib},E_{rot})$ and $P(E,E') = P(E_{vib},E_{rot};E'_{vib},E'_{rot})$]. However, the solution of the two-dimensional equation is formidable, requiring a 4-fold summation. The problem becomes more tractable if the probability functions for vibrational and rotational-energy transfer are assumed to be independent of each other, thereby enabling $P(E_{vib},E_{rot};E'_{vib},E'_{rot})$ to be separated into vibrational and rotational parts according to eq 27:

$$P(E_{vib},E_{rot};E'_{vib},E'_{rot}) = P_{vib}(E_{vib},E'_{vib})\, P_{rot}(E_{rot},E'_{rot}) \quad (27)$$

Furthermore, the exponential down-step probability function is equivalent to the "unrestricted ΔJ exponential model", which was found to provide the best fit to rotational relaxation data for excited HCl.[45] Therefore, $P_{down}(E;E')$ is used to describe both vibrational and rotational-energy transfer in this study.

Independence of the vibrational and rotational probability functions implies that the corresponding degrees of freedom are decoupled during simultaneous energy transfer, or alternatively, that each collision results in exclusive rotational or vibrational excitation. Although the physical reality of such assumptions

about these processes is subject to question, detailed calculations[46] comparing simultaneous vibrational−rotational-energy transfer with exclusive vibrational or rotational transfer indicate marginal differences in the final overall dissociation rate. Furthermore, a simple model which represents k_{diss} as the sum of vibrational and rotational dissociation rates has given results in good agreement with experiment. That is, adiabatic rotations increase the purely vibrational dissociation rate by a factor equal to the sum of a series of purely rotational dissociation rates (having threshold rotational dissociation energy given by the inverse of eq 26, i.e., $E_{rot}^{max}(E_{vib})$, over all vibrational levels below the critical energy. The upper limit of k_{diss}, for dissociations occurring as the result of either purely vibrational activation or the combination of vibrational and rotational activation, corresponds to situations in which equilibrium energy distributions are present. Thus, for the energy-transfer probabilities given by eqs 11 and 12, the maximum vibrational dissociation rate $k_{diss_{max}}^{vib}$ is

$$k_{diss_{max}}^{vib} = \frac{\omega}{Q_{vib}} \sum_{E_{vib}=0}^{\infty} \rho_{vib} \exp\left(\frac{-E_{vib}}{kT_{eff}}\right) \tag{28}$$

and the maximum rovibrational dissociation rate $k_{diss_{max}}^{rovib}$ is

$$k_{diss_{max}}^{rovib} = k_{diss_{max}}^{vib}\left[1 + \frac{\omega}{Q_{vib}\, k_{diss_{max}}^{vib}} \sum_{E_{vib}=0}^{E_0} \rho_{vib} \exp\left(\frac{-[E_{vib} + E_{rot_{max}}(E_{vib})]}{kT_{eff}}\right)\right] \tag{29}$$

where Q_{vib} is the vibrational partition function and ρ_{vib} is the density of vibrational states. Given the very high unimolecular dissociation rates for diatomic ions and relatively inefficient energy transfer associated with monatomic collision events, it is improbable that equilibrium conditions exist during diatomic ion CID in the quadrupole ion trap. However, factoring the vibrational−rotational probability according to eq 16 allows the nonequilibrium two-dimensional master equation to be solved by methods similar to those employed for the numerical solution of the corresponding one-dimensional (vibrational) master equation. One such technique, termed the exact stochastic method (ESM),[47] monitors the evolution of ion internal energy over a series of ion−neutral collisions, with the intervals between collisions and the direction and magnitude of the energy change at each collision being determined via a Monte Carlo technique.

Random Walk Procedure. In the ESM, the random time interval τ between ion−neutral collisions is

$$\tau = \frac{1}{\omega} \ln\left(\frac{1}{r}\right) \tag{30}$$

where r is a random number from the unit-interval distribution (equal probability for any number between 0 and 1). The ion−neutral hard-sphere collision frequency was calculated from eq 31:

$$\omega = N\pi\sigma^2 \sqrt{\frac{8kT_{eff}}{\pi\mu}} \tag{31}$$

N is the neutral number density, μ is the reduced mass of the collision pair, and the Ne−TaO^+ hard-sphere collision cross-section $\pi\sigma^2$ was assigned as 39 Å^2 on the basis of radii of 1.85 and 1.7 Å for TaO^+ and Ne, respectively.

Initial vibrational and rotational energies for the intact diatomic ion are randomly chosen from a 300 K Boltzmann distribution. The ion is then assigned a specific internal temperature at which it undergoes collisional activation and deactivation during a random walk in energy space. Each ion−neutral collision is assumed to result in one of three events: (1) an increase, (2) a decrease, or (3) no change in energy, for rotational as well as for vibrational processes because they are assumed to be independent of each other. The direction of energy change resulting from each collision is determined by comparing another random number of the same type to the probability for an energy down-step $P_{downstep}$ as given by eq 32:

$$P_{downstep} = \frac{\int_E^{E'} \exp\frac{-(E - E')}{\alpha}\, dE'}{C} = \frac{kT_{int} + \alpha}{2kT_{int} + \alpha}, \quad E' < E \tag{32}$$

Note that for each collision two separate comparisons (each with a different random number) are required. The final step in the simulation of energy transfer, the randomization of the energy-step size for each collision, is accomplished by inverting the exponential energy-transfer probability function to give eq 33:

$$\Delta E_{down} = -\alpha \ln(r) \tag{33}$$

where ΔE_{down} represents the random energy down-step size and separate determinations are made for vibrational and rotational-energy transfers. Energy down-steps are constrained by assuming that any collision for which $\Delta E_{down} > E$ is elastic and no energy change occurs. Similarly, replacing α with β in eq 33 allows the size of the vibrational and rotational energy up-steps to be randomized. Although it is doubtful that equilibrium conditions exist during diatomic ion CID in the quadrupole ion trap, as noted above, simulations were also performed for rotational equilibrium conditions to provide an upper limit for expected dissociation rates (vide infra). For such simulations, the rotational energy was determined by random sampling from a Boltzmann rotational-energy distribution.

Dissociation kinetics can be simulated by terminating ion trajectories in energy space when the internal energy exceeds the (rotational-energy-dependent) barrier for dissociation given in eq 26, a procedure sometimes referred to as the sudden-death approximation. The critical dissociation energy for TaO^+, $E_0(Ta^+-O) = 7.63 \pm 0.15$ eV, was derived from the neutral TaO bond dissociation energy, $E_0(Ta-O) = 8.35 \pm 0.13$ eV, and the IEs of Ta, IE(Ta) = 7.89 eV, and TaO, IE(TaO) = 8.61 ± 0.02 eV, using eq 34:

$$E_0(Ta^+ - O) = E_0(Ta - O) + IE(Ta) - IE(TaO) \tag{34}$$

As noted above, this procedure assumes the unimolecular dissociation rate of an ion with an internal energy exceeding the threshold for fragmentation is much faster than the deactivation rate; the assumption is most valid for diatomic ions because their lifetimes at energies above the dissociation threshold is on the order of a vibrational period. Performing a series of many such random walks (i.e., simulating the dissociations of many ions) and then plotting the number of undissociated parent ions as a function of excitation time yields a simulated CID dissociation rate curve. Ensemble averaging of the histogrammed internal energy data from each random walk enables the time-dependent internal energy distribution of the ion population at

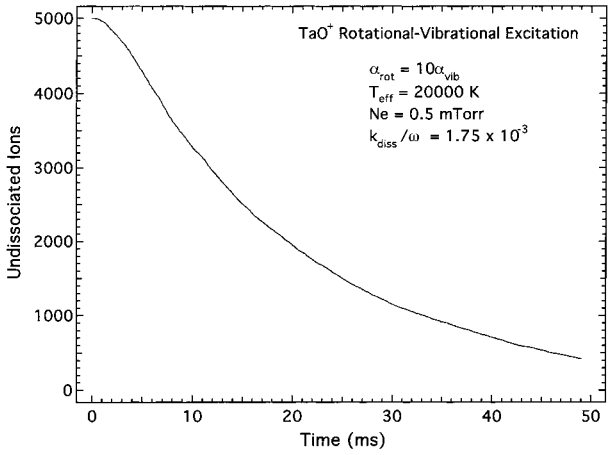

Figure 1. Number of undissociated TaO^+ ions at 20 000 K (α_{vib} = 0.135 eV, $\alpha_{rot} = 10\alpha_{vib}$) as a function of time, from which the dissociation rate can be derived.

T_{eff} to be obtained. In addition, because vibrational- and rotational-energy changes are simulated and tracked independently, the vibrational and rotational distributions can be examined separately.

Results and Discussion

Using the methods described above, simulations of TaO^+ dissociation via multiple collisions with Ne (0.5 mTorr, 300 K) were performed for 10^4 ions at various assigned values of T_{eff} and the corresponding vibrational-energy-transfer parameter α_{vib} (as determined from eq 25). For each T_{eff}, the effects of rotational dissociation were also considered by using rotational-energy transfer parameters likely to represent the extremes of such experiments, that is, for $\alpha_{rot} = \alpha_{vib}$ and for rotational equilibrium, as well as for an intermediate condition, $\alpha_{rot} = 10\alpha_{vib}$. Figure 1, for example, shows a plot of the number of undissociated TaO^+ ions as a function of time for $T_{eff} = 20\,000$ K ($\alpha_{vib} = 0.135$ eV and $\alpha_{rot} = 10\alpha_{vib}$). Dissociation rates k_{diss} were obtained from the random walk simulations via the slope of the $-\ln([TaO^+]_t/[TaO^+]_0)$ vs time curves as determined using linear least-squares fitting. Because collisional energy transfer is rate-limiting at the Ne pressure used in these simulations, as well as at buffer gas pressures normally used for ion trap CID, the simulated k_{diss} values are scaled by the collision frequency. For example, eq 31 yields a collision frequency of 3.0×10^4 s^{-1} at 20 000 K.

Figure 2 compares the simulated dissociation rates determined in the above manner over the range of assigned T_{eff} values used in this work. As noted previously, diatomic dissociation can occur over a range of vibrational energies less than the critical energy because rotational energy can be channeled into vibrational motion as the interatomic distance increases. Consequently, incorporation of rotational-energy transfer in the simulations is seen to result in increased dissociation rates relative to purely vibrational-energy transfer. For example, at 20 000 K when rotational-energy transfer is excluded, k_{diss}/ω (6.08×10^{-5}) is somewhat less than that obtained at the lower extreme of rotational-energy transfer $\alpha_{rot} = \alpha_{vib}$ (3.03×10^{-4}) and significantly less than at $\alpha_{rot} = 10\ \alpha_{vib}$ (1.75×10^{-3}) and at rotational equilibrium (5.43×10^{-3}). For comparison purposes, the maximum vibrational dissociation rate $k^{vib}_{diss_{max}}/\omega$ from eq 28 is 1.16×10^{-2} and the maximum rovibrational dissociation rate $k^{rovib}_{diss_{max}}/\omega$ from eq 29 is 4.05×10^{-2}.

Experimental k_{diss}/ω values for CID of TaO^+ in the quadrupole ion trap are plotted vs peak-to-peak resonance excitation

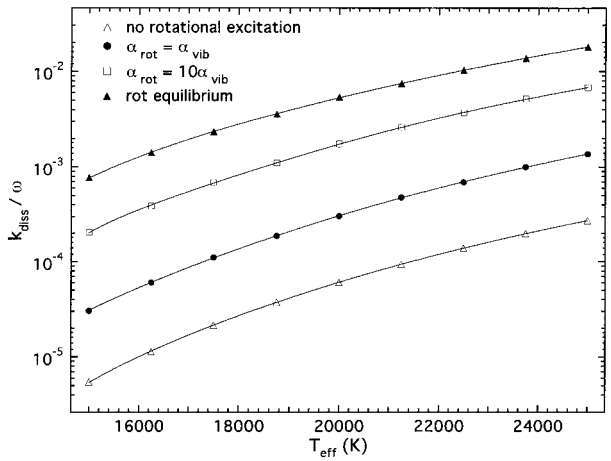

Figure 2. Simulated dissociation rates for TaO/Ne at a Ne pressure of 0.5 mTorr as a function of effective temperature for rotational−vibrational dissociation and for vibrational dissociation only.

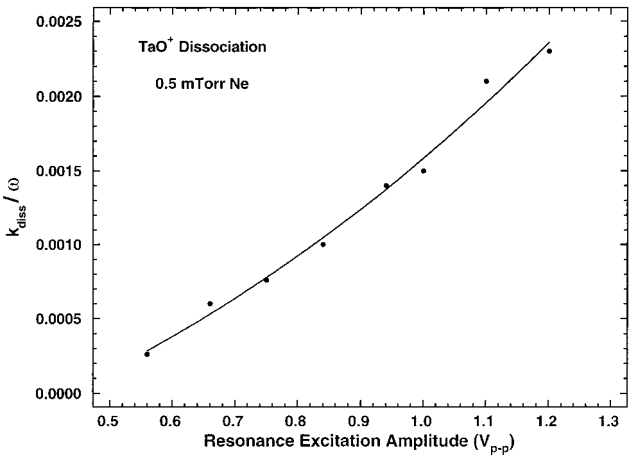

Figure 3. Experimental dissociation rates for TaO^+ undergoing CID via resonance excitation in 0.5 mTorr of Ne buffer gas.

voltage in Figure 3. Over the range of resonance excitation voltages used, experimentally measured k_{diss}/ω values ranged from about 2.6×10^{-4} to 2.3×10^{-3}. Comparison of the experimental dissociation rates with those determined from simulations can provide an estimate of T_{eff} values attainable by collisional activation of strongly bound diatomic ions in a quadrupole ion trap. For example, k_{diss}/ω for a resonance excitation voltage of 1 V_{p-p} was 1.5×10^{-3}. If the simulated k_{diss}/ω curves in Figure 2 for $\alpha_{rot} = \alpha_{vib}$ and rotational equilibrium are assumed to represent the extremes of rotational-energy transfer, then the corresponding T_{eff} value at that voltage is bracketed by approximately 16 000 (rotational equilibrium) and 25 000 K ($\alpha_{rot} = \alpha_{vib}$), with an intermediate value of about 19 000 K ($\alpha_{rot} = 10\alpha_{vib}$). The overall range of observed experimental k_{diss}/ω values is bracketed by corresponding T_{eff} values extending from about 13 500 to 18 000 K (rotational equilibrium) and from approximately 19 500 to 27 000 K ($\alpha_{rot} = \alpha_{vib}$); the T_{eff} range is about 15 500−21 000 K for $\alpha_{rot} = 10\alpha_{vib}$.

It is interesting to compare the T_{eff} estimates deduced herein by the correlation of experimental and simulated dissociation rates (vide supra) with those generated via a software package, ITSIM, developed by Cooks' group to simulate ion processes in quadrupole ion traps.[48] Ion trajectories are calculated numerically in ITSIM as solutions to Newton's equations for ion motion in electric fields which result from various ion trap operating conditions and electrode geometries. T_{eff} values, which

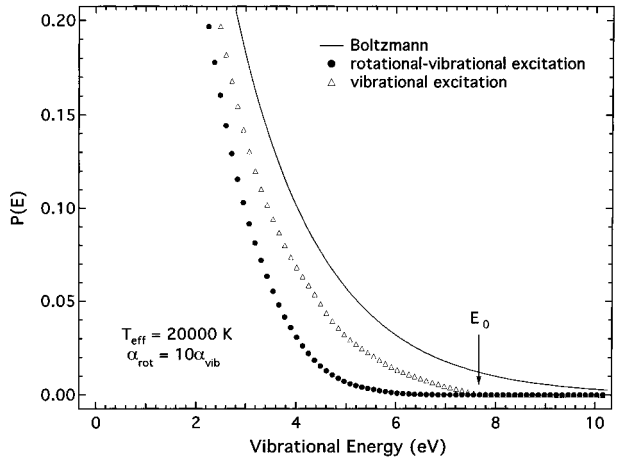

Figure 4. Steady-state vibrational-energy distributions from ESM simulations of TaO^+/Ne dissociation at $T_{eff} = 20\,000$ K ($\alpha_{vib} = 0.135$ eV, $\alpha_{rot} = 10\alpha_{vib}$). The corresponding Boltzmann energy distribution for TaO^+ ions fragmenting under equilibrium conditions is plotted as well.

represent the total random kinetic energy available to the diatomic internal degrees of freedom, are subsequently calculated from the relative ion−neutral velocities. For ITSIM simulations using the Ne pressure (0.5 mTorr), resonance excitation frequency (226 kHz), and range of excitation voltages (0.56−1.2 V_{p-p}) employed in the TaO^+ dissociation experiments, the predicted T_{eff} values (∼15 000−24 000 K) are in good agreement with the estimates made above. Dissociation rates could not be compared because our version of ITSIM did not incorporate simulated fragmentation processes.

It is notable that besides increasing k_{diss} rotational dissociation also has an effect on the internal energy distribution of a dissociating TaO^+ ion population, which reaches steady state during the linear portion of the $-\ln([TaO^+]_t/[TaO^+]_0)$ vs time curve. Figure 4 compares the TaO^+ steady-state vibrational-energy distribution ($T_{eff} = 20\,000$ K, $\alpha_{rot} = 10\alpha_{vib}$) following 1500 collisions for rotational−vibrational dissociation and vibrational dissociation only; the curves have been normalized. The corresponding Boltzmann energy distribution for TaO^+ ions fragmenting under equilibrium conditions is plotted as well. Because dissociation occurs under nonequilibrium conditions for such situations, the ion population cannot be maintained at the equilibrium Boltzmann distribution. Furthermore, examination of the distributions reveals that rotational-energy transfer contributes to increased depopulation of vibrational energies as compared with vibration excitation only because the threshold for vibrational dissociation is a function of rotational energy. For example, the normalized ion populations at 7 and 6 eV are 27.1% and 43.2%, respectively, of the equilibrium populations for the purely vibrational simulation, whereas the same populations are 99.7% and 96.9% depopulated, respectively, for rotational−vibrational dissociation.

Conclusions

The relationship between ion activation conditions and ion internal temperatures for high-mass polyatomic ions is the subject of ongoing research[25,28,49−51], so it is interesting to consider the results for dissociation of strongly bound diatomic ions within that context. A recent ion activation study involving protonated leucine-enkephalin, a five-residue polypeptide ion, demonstrated a nearly 400 K increase in internal temperature by the use of resonance excitation and helium as the buffer gas.[28] Although achievement of higher internal temperatures was precluded by ion ejection from the ion trap, such an increase in temperature still was sufficient to drive dissociation rates to nearly 100 s^{-1}. Correlation of internal temperatures with resonance excitation parameters was achieved by the use of Arrhenius parameters for leucine-enkephalin previously obtained via thermal dissociation rate measurements. The determination of ion internal temperatures for various ion activation techniques via that method is straightforward when the parent ion internal energy distribution is Boltzmann. Such situations exist when collisional activation and deactivation rates are far greater than unimolecular dissociation rates, a condition termed the rapid energy exchange limit. However, the probability of rapid energy exchange conditions prevailing diminishes as the internal temperature increases and the number of degrees of freedom of the parent ion decreases. Strongly bound diatomic ions represent the extreme case because far higher effective temperatures are required to effect dissociation which is expected to occur at vibrational frequencies, the result being a significant deviation from a Boltzmann internal energy distribution. Although experimental results presented here suggest that such temperatures are achievable via resonance excitation, the correlation of effective temperatures with experimental parameters is problematic because heating the buffer gas to such temperatures so as to achieve dissociation is obviously an impractical approach.

Given the experimental difficulties associated with estimating the internal temperatures of diatomic ions undergoing collisional activation in the ion trap, we have approached the problem via simulation techniques. For diatomic dissociations, conservation of the angular momentum requires rotational energy to be released into vibrational motion as the interatomic distance increases. Consequently, the threshold energy for vibrational dissociation is a decreasing function of increasing rotational energy enabling fragmentation to occur over a range of vibrational energies less than the binding strength of the diatomic. Thus, in addition to vibrational-energy transfer, it is important to incorporate rotational-energy transfer in CID simulations to improve the accuracy of predicted dissociation rates. The simulation results reported here, which take both T−V and translational−rotational-energy transfer into consideration, suggest that effective temperatures in the tens of thousands of degrees are required to dissociate a strongly bound diatomic ion such as TaO^+, even under rotational equilibrium conditions. Furthermore, the experimental data indicate that collisional activation via resonance excitation in a quadrupole ion trap appears capable of accessing the necessary temperatures. Examination of the internal energy distribution also reveals that rotational-energy transfer contributes to increased depopulation of vibrational energies as compared with vibration excitation only.

Despite the remarkably high internal temperatures apparently achievable by collisional activation via ion trap resonance excitation, the average internal energy E_{avg_int} of TaO^+ is comparable to that present in much larger polyatomics during CID because of the large difference in degrees of freedom. For

$$E_{avg\_int} = \sum_{n=1}^{\text{number of oscs}} \frac{g_n h\nu_n}{\exp\left[\frac{h\nu_n}{kT_{int}}\right] - 1}$$

$\nu \equiv$ oscillator frequency, g ≡ oscillator degeneracy

example, in this study, the predicted internal temperature for TaO^+ (1 internal degree of freedom) dissociating at 30 s^{-1} is

about 20 000 K; the corresponding average internal energy at that temperature is 1.67 eV. In comparison, an internal temperature of approximately 610 K, corresponding to 3.61 eV average internal energy, was required to drive CID of protonated leucine-enkephalin (219 internal degrees of freedom) at the same rate. Furthermore, it is notable that even at such high effective temperatures the probability for formation of doubly charged tantalum oxide ions (TaO^{2+}) via electronic excitation of TaO^+ is extremely low. The principle generally used to relate such excitation probability to ion kinetic energy is the adiabatic criterion of Massey[52] which asserts that the maximum transition probability occurs when the collision and electronic transition times are comparable. Expressed in terms of the relative ion−neutral velocity corresponding to the maximum transition probability v_{max_prob} the Massey adiabatic criterion is approximated by

$$v_{max\_prob} \approx \frac{a_{interact}\Delta E}{h}$$

where $a_{interact}$ is the effective interaction distance, ΔE is the difference in energy between states, and h is Planck's constant. When the above equation is applied to the formation of TaO^{2+}, the first ionization energy of TaO^+ (8.61 eV) can be substituted for ΔE (the second ionization energy is unavailable to our knowledge, but can be assumed greater than or equal to the first ionization energy) and 5 Å can be taken as the typical interaction distance. The resulting v_{max_prob} is 1.0×10^8 cm s^{-1} (1.0×10^5 eV) as compared with the relative TaO^+−Ne velocity of 5.2×10^5 cm s^{-1} (2.6 eV) at $T_{eff} = 20\,000$ K (obtained via eq 22).

Acknowledgment. We thank W. B. Whitten for suggestions on manuscript enhancement prior to submission. This research was sponsored by the Division of Chemical Sciences, Geosciences, and Biosciences, Office of Basic Energy Sciences, U.S. Department of Energy, under Contract DE-AC05-00OR22725 with Oak Ridge National Laboratory, managed and operated by UT-Battelle, LLC.

References and Notes

(1) McLuckey, S. A.; Van Berkel, G. J.; Goeringer, D. E.; Glish, G. L. *Anal. Chem.* **1994**, *66*, 689A.
(2) Quarmby, S. T.; Yost, R. A. *Int. J. Mass Spectrom.* **1999**, *190*, 81.
(3) Brodbelt, J. S. In *Practical Aspects of Ion Trap Mass Spectrometry*; March, R. E., Todd, J. F. J., Eds.; CRC Press: New York, 1995; Vol. I, Chapter 5.
(4) Louris, J. N.; Amy, J. W.; Ridley, T. Y.; Cooks, R. G. *Int. J. Mass Spectrom. Ion Processes* **1989**, *88*, 97.
(5) Louris, J. N.; Cooks, R. G.; Syka, J. E. P.; Kelley, P. E.; Stafford, G. C., Jr.; Todd, J. F. J. *Anal. Chem.* **1987**, *59*, 1677.
(6) McLuckey, S. A.; Goeringer, D. E..; Glish, G. L. *Anal. Chem.* **1992**, *64*, 4, 1455.
(7) Paradisi, C.; Todd, J. F. J.; Vettori, U. *Org. Mass Spectrom.* **1992**, *27*, 1210.
(8) Curcuruto, O.; Fontana, S.; Traldi, P.; Celon, E. *Rapid Commun. Mass Spectrom.* **1992**, *6*, 322.
(9) Traldi, P.; Catinella, S.; March, R. E.; Creaser, C. S. In *Practical Aspects of Ion Trap Mass Spectrometry*; March, R. E., Todd, J. F. J., Eds.; CRC Press: New York, 1995; Vol. I, Chapter 7.
(10) Qin, J.; Chait, B. T. *Anal. Chem.* **1996**, *68*, 2108.
(11) Lammert, S. A.; Cooks, R. G. *Rapid Commun. Mass Spectrom.* **1992**, *6*, 528.
(12) Wang, M.; Schachterle, S.; Wells, G. *J. Am. Soc. Mass Spectrom.* **1996**, *7*, 668.
(13) McLuckey, S. A.; Glish, G. L.; Duckworth, D. C.; Marcus, R. K. *Anal. Chem.* **1992**, *64*, 1606.
(14) Van Berkel, G. J.; Glish, G. L.; McLuckey, S. A. *Anal. Chem.* **1990**, *62*, 1284.
(15) McLuckey, S. A.; Glish, G. L.; Van Berkel, G. J. *Anal. Chem.* **1991**, *63*, 1971.
(16) Stephenson, J. L., Jr.; McLuckey, S. A. *Anal. Chem.* **1998**, *70*, 3533.
(17) Schnier, P. D.; Price, W. D.; Jockusch, R. A.; Williams, E. R. *J. Am. Chem. Soc.* **1996**, *118*, 7178.
(18) Price, W.D.; Williams, E. R. *J. Phys. Chem.* **1997**, *101*, 8844.
(19) Thölmann, D.; Tonner, D. S.; McMahon, T. B. *J. Phys. Chem.* **1994**, *98*, 2002.
(20) Dunbar, R. C. *J. Phys. Chem.* **1994**, *98*, 8705.
(21) Dunbar, R. C.; McMahon, T. B. *Science* **1998**, *279*, 194.
(22) McLuckey, S. A.; Goeringer, D. E. *J. Mass Spectrom.* **1997**, *32*, 461.
(23) Goeringer, D. E.; McLuckey, S. A. *J. Chem. Phys.* **1996**, *104*, 2214.
(24) Goeringer, D. E.; McLuckey, S. A. *Rapid Commun. Mass Spectrom.* **1996**, *10*, 328.
(25) Asano, K. G.; Goeringer, D. E.; McLuckey, S. A. *Int. J. Mass Spectrom.* **1999**, *185/186/187*, 207.
(26) Penner, A. P.; Forst, W. *Chem. Phys.* **1975**, *11*, 243.
(27) Stace, A. J. *Mol. Phys.* **1979**, *38*, 155.
(28) Goeringer, D. E.; Asano, K. G.; McLuckey, S. A. *Int. J. Mass Spectrom.* **1999**, *182/183*, 275.
(29) Duckworth, D. C.; Barshick, C. M.; Smith, D. H.; McLuckey, S. A. *Anal. Chem.* **1994**, *66*, 92.
(30) Duckworth, D. C.; Smith, D. H.; McLuckey, S. A. *J. Anal. At. Spectrosc.* **1997**, *12*, 43.
(31) Barinaga, C. J.; Koppenaal, D. W. *Rapid Commun. Mass Spectrom.* **1994**, *8*, 71−76.
(32) Koppenaal, D. W.; Barinaga, D. W.; Smith, M. R. *J. Anal. At. Spec.* **1994**, *9*, 1053.
(33) Eiden, G. C.; Barinaga, C. J.; Koppenaal, D. W. *J. Anal. At. Spec.* **1996**, *11*, 317.
(34) Eiden, G. C.; Barinaga, C. J.; Koppenaal, D. W. *J. Am. Soc. Mass Spectrom.* **1996**, *7*, 1161.
(35) Barinaga, C. J.; Eiden, G. C.; Alexander, M. J.; Koppenaal, D. W. *Fresenius' J. Anal. Chem.* **1996**, *355*, 487.
(36) Duckworth, D. C.; Goeringer, D. E.; McLuckey, S. A. *J. Am. Soc. Mass Spectrom.*, in press.
(37) Stafford, G. C., Jr.; Kelley, P. E.; Syka, J. E. P.; Reynolds, W. E.; Todd, J. F. J. *Int. J. Mass Spectrom. Ion Processes* **1984**, *60*, 85.
(38) McLuckey, S. A.; Goeringer, D. E.; Glish, G. L. *J. Am. Soc. Mass Spectrom.* **1991**, *2*, 11.
(39) Goeringer, D. E.; Asano, K. G.; McLuckey, S. A.; Hoekman, D.; Stiller, S. E. *Anal. Chem.* **1994**, *66*, 313.
(40) Tardy, D. C.; Rabinovitch, B. S. *Chem. Rev.* **1977**, *11*, 369.
(41) Forst, W. *Theory of Unimolecular Reactions*; Academic Press: New York, 1973; Chapter 8.
(42) Mahan, B. H. *J. Chem. Phys.* **1970**, *52*, 5221.
(43) Shobatake, K.; Rice, S. A.; Lee, Y. T. *J. Chem. Phys.* **1973**, *59*, 2483.
(44) Kelley, J. D.; Wolfsberg, M. *J. Chem. Phys.* **1966**, *44*, 324.
(45) Polanyi, J. C.; Woodall, K. B. *J. Chem. Phys.* **1972**, *56*, 1563.
(46) Pritchard, H. O. In *Reaction Kinetics, A Specialist Periodical Report*; Ashmore, P. G., Senior Reporter; The Chemical Society: London, U.K., 1975; Vol. 1, p 243 ff.
(47) Gillespie, D. T. *J. Phys. Chem.* **1977**, *81*, 2340.
(48) Bui, H. A.; Cooks, R. G. *J. Mass Spectrom.* **1998**, *33*, 297.
(49) Asano, K. G.; Butcher, D. J.; Goeringer, D. E.; McLuckey, S. A. *J. Mass Spectrom.* **1999**, *34*, 691.
(50) Asano, K. G.; Goeringer, D. E.; Butcher, D. J.; McLuckey, S. A. *Int. J. Mass Spectrom.* 1999, *190/191*, 281.
(51) Butcher, D. J.; Asano, K. G.; Goeringer, D. E.; McLuckey, S. A. *J. Phys. Chem. A* **1999**, *103*, 8664.
(52) Massey, H. S. W. *Rep. Prog. Phys.* **1949**, *12*, 3279.